

Biomolecular shape and interactions determined by fluorescence correlation spectroscopy

J. Langowski, M. Wachsmuth, K. Rippe and M. Tewes

Deutsches Krebsforschungszentrum, Division Biophysics of Macromolecules
Im Neuenheimer Feld 280, D-69120 Heidelberg, Germany

1. Introduction

The quantitative characterization of biomolecular interactions is of fundamental importance for our understanding of cellular mechanisms. Various methods have been applied to measure the thermodynamics and kinetics of such interactions, but many of those commonly used such as gel shift, nitrocellulose filter binding, or surface plasmon resonance are restricted to systems that are bound to or confined within some kind of matrix.

For measuring binding parameters with an accuracy that allows to distinguish between different binding mechanisms, cooperativity etc., one needs to determine these quantities free in solution. Classical titration methods which monitor an optical parameter such as absorbance, fluorescence intensity or depolarization, or circular dichroism, have the disadvantage that often large quantities are needed and binding constants greater than 10^8 M^{-1} can be measured only with great difficulty because of the limited sensitivity.

Fluorescence correlation spectroscopy (FCS) is a method that has recently gained importance for the measurement of interactions between biomolecules in solution. It is used to determine the concentrations and hydrodynamic properties of fluorescent molecules by analyzing their number fluctuations.

This technique and its theoretical foundations have been described some time ago¹⁻³, but routine measurements of biomolecular interactions have become possible only by recent improvements^{4,5}: these include the use of confocal optics for excitation and detection, and avalanche photodiode detectors that offer a quantum efficiency $> 50\%$ in the red range of the visible spectrum (a factor of ten over that of typical photomultipliers).

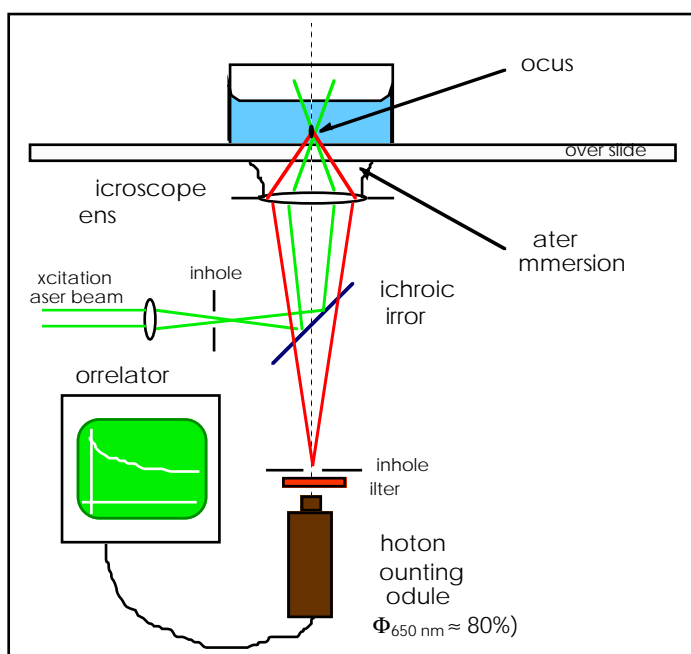


Fig. 1: Schematic principle of the FCS method.

The principle of the method is shown schematically in Fig. 1. The fluorescent molecules are excited in a very small detection volume ($\approx 1 \text{ fl}$) with a laser beam focused through a microscope lens. The emitted fluorescence is detected through the same optics; excitation and emission wavelengths are separated by a dichroic mirror and filters.

Very small concentrations ($< 1 \text{ pM}$) may be detected because individual fluorescent particles will give clearly distinguishable bursts of fluorescence intensity above the background arising from detector noise, Raman scattering and optical imperfections. The amplitudes and characteristic time scales of the measured fluctuations are directly connected to macroscopic properties such as particle concentration or diffusion constants; therefore FCS can be used to measure concentrations and sizes of fluorescent molecules in solutions.

As an example, interactions between molecules may manifest themselves in a decrease of the measured concentration: when dimers are formed, only half as many particles are present in the solution. In parallel, the mean residence time of the molecules in the observation volume will increase because of their slower diffusion.

Due to the small focus of the laser beam, measurements inside biological objects also become possible. A typical high-resolution microscope lens has a focal spot of 300 nm diameter and 1.5 μm length, such that diffusion processes inside cells or organelles can be probed in a position-dependent manner. FCS has for instance been used to probe chromatin in the cell nucleus⁶.

Another recent development in FCS is the use of two-color detection with cross-correlation (FCCS; Fig.2)^{7,8}. Here emitted light from the same focal volume is detected at two wavelengths, and particles which fluoresce at both wavelengths will give simultaneous bursts of intensity in the two channels. This correlated emission is detected by computing a cross correlation function. FCCS is a convenient means to show binding between two ligands labeled with different fluorophores because the complex will show correlated fluorescence at the two wavelengths.

2. Theoretical foundation of FCS

2.1. Concentration fluctuations in small systems

In a solution of concentration c , the fluctuation of the instantaneous number of solute molecules N in a given volume element V is $\langle \delta N^2 \rangle = \langle N \rangle$, where $\langle N \rangle = c \cdot V$ is the average number of molecules in V and $\langle \delta N^2 \rangle = \langle (N - \langle N \rangle)^2 \rangle$ the mean squared fluctuation. The time dependence of the fluctuations is directly related to the diffusion coefficient of the molecule (see below). By observing the concentration fluctuation of a solute in a very small volume of known size, one can thus determine its concentration and its diffusion coefficient.

Let us assume we measure the fluorescence of a 10^{-9} M rhodamin solution in volume elements of various sizes. Table 1 shows the absolute and relative number fluctuations for this case. In a classical fluorescence spectrometer the typical observation volume is of the order of 1 ml. It is easily seen that at this sample size no observable fluctuation is expected. If one, however, measures the fluorescence of the same solution in a smaller volume, the fluctuations become increasingly important until they reach the size of the fluorescence

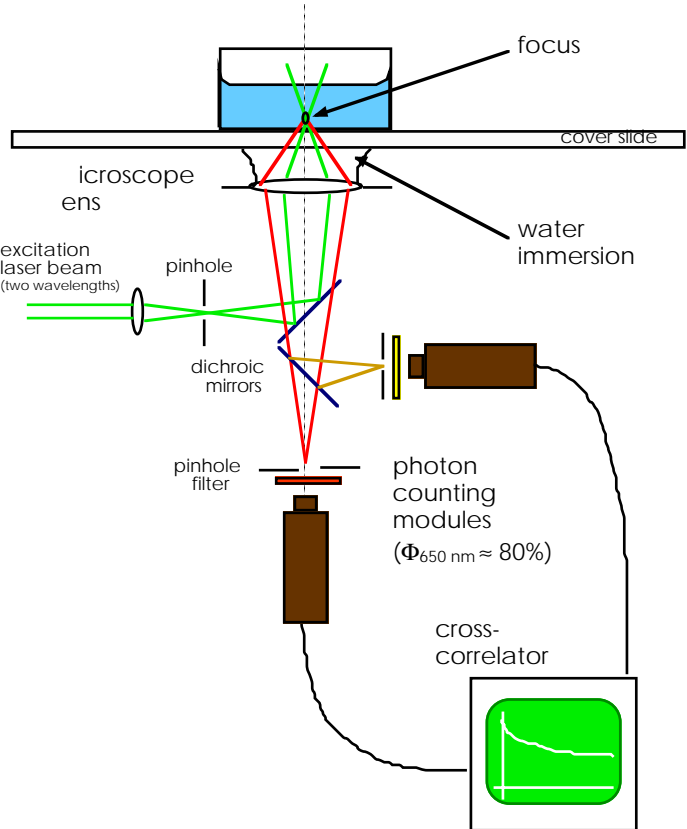


Fig. 2: Principle of two-color FCCS.

Table 1: Number fluctuations in a 1 nM solution as a function of volume

Size [mm]	Volume [l]	# of particles	ΔN	$\Delta N/N [\%]$
10	10^{-3}	$6.023 \cdot 10^{11}$	776080	0.00013
1	10^{-6}	$6.023 \cdot 10^8$	24541	0.0041
0.1	10^{-9}	$6.023 \cdot 10^5$	776	0.129
0.01	10^{-12}	602.3	24.5	4.075
0.001	10^{-15}	0.6023	0.776	128.9

signal itself at a sample size of 1 fl; here, less than one molecule is present in the observation volume on average. The characteristics of the fluorescence fluctuations and their relation to molecular properties are summarized in the following.

2.1.1. Autocorrelation, one species

The primary data obtained in an FCS measurement is the time-dependent fluorescence intensity $F(t)$, which is proportional to the number of particles in the observation volume at time t . The autocorrelation function of $F(t)$ contains all relevant information relating to the diffusion of the fluorophores. The normalized autocorrelation function $G(\tau)$ is computed as

$$G(\tau) = \frac{\langle F(t)F(t + \tau) \rangle}{\langle F(t) \rangle^2} \quad (1)$$

For obtaining quantities such as diffusion coefficients, concentrations or reaction rate constants, one has to fit a theoretical correlation function to the measured $G(\tau)$ which is based on a model that contains these quantities as free parameters. For a solution of a single fluorescent species with diffusion coefficient D and molar concentration c and for Gaussian profiles for the excitation intensity and detection efficiency, $G(\tau)$ evaluates to ⁵:

$$G(\tau) = \frac{1}{cV_{\text{eff}}} \left(1 + \frac{4D\tau}{w_0^2} \right)^{-1} \left(1 + \frac{4D\tau}{z_0^2} \right)^{-1/2} + 1 \quad (2)$$

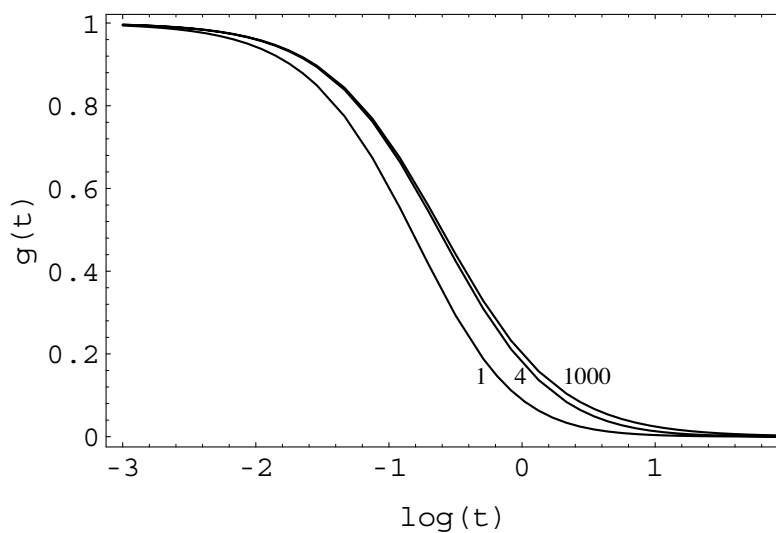


Fig. 3: Influence of the structure factor κ on the FCS autocorrelation function. Three curves are displayed for the same diffusion time τ and $\kappa = 1, 4, 1000$. Since $\kappa \geq 4$ for typical confocal optics, the relevant range in practice is between the rightmost two curves.

Here V_{eff} is the effective observation volume which depends on the geometry of the focus for excitation and emission, w_0 and z_0 are the half-widths of the focus in the x-y plane (the observation plane of the lens) and in the z-direction, respectively.

V_{eff} , w_0 and z_0 can be measured independently by calibration with a solution of a fluorophore of known concentration and diffusion coefficient. If only relative changes are of interest, one can use the average particle number $N = cV_{\text{eff}}$ and an effective diffusion time $\tau_{\text{diff}} = w_0^2/4D$ as parameters:

$$G(\tau) = \frac{1}{N} \left(1 + \frac{\tau}{\tau_{\text{diff}}} \right)^{-1} \left(1 + \frac{\tau}{\tau_{\text{diff}} \kappa^2} \right)^{-1/2} + 1 \quad (3)$$

κ (also called the structure factor) is the axial ratio of the observation volume, z_0/w_0 .

For a high aperture lens ($NA = 1.2$) at optimal alignment κ typically ranges between 4 and 6. As can be seen in Fig. 3, the influence of κ on the shape of the correlation function is rather small in this region, and errors on the measured $G(\tau)$ that are due to insufficient statistics or slowly diffusing components such as dust or aggregates may easily lead to a wrong estimate for κ . In a typical FCS experiment one would therefore determine κ on a monodisperse solution of a known fluorophore and keep its value fixed for the measurements of the unknown sample.

2.1.1.1 Concentration determination

The intercept of the FCS autocorrelation function $G(\tau)$ is inversely proportional to the number of particles in the focal volume, and thus to their concentration. In practice, deviations from this ideal behavior are found at very high and very low concentrations. At low concentrations these deviations are due to the background which becomes comparable to the fluorescence signal, and which is caused by incomplete suppression of the excitation light, detector dark counts and background fluorescence. At a particle concentration c the measured particle number N in the presence of background is then

$$N = cV_{\text{eff}} \left(1 + \frac{v}{c}\right)^2 \quad (4)$$

where $v = \langle U \rangle / f$ is the ratio of the background signal to the normalized fluorescence intensity of the fluorophor. Fig. 4 shows this effect on a solution of Texas Red - cystein over a concentration range of 50 fM to 1 μ M.

Deviations at high concentrations are due to slow fluorescence intensity fluctuations which can arise from slow adsorption of the dye to the cuvette walls or to larger particles (e.g. dust). If the concentration of the dye is known, the effective detection volume V_{eff} and the relative background v can be obtained from a fit to the curve in Fig. 4. With the two different lenses used, these parameters are $V_{\text{eff}} = 0.26 \text{ fl}$ and $v = 2.4 \cdot 10^{-10} \text{ M}$ for the 60x/1.2W lens and $V_{\text{eff}} = 1.21 \text{ fl}$ and $v = 5.5 \cdot 10^{-10} \text{ M}$ for the 60x/0.9W lens.

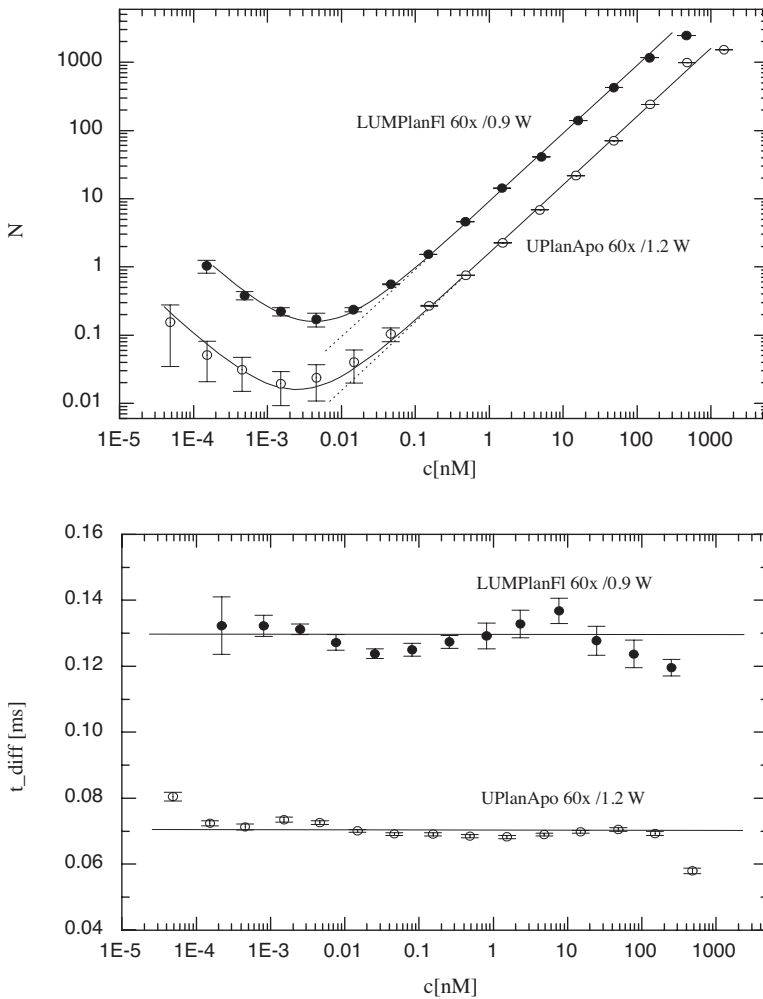


Fig. 4: Observed particle number N and diffusion time t_{diff} as a function of sample concentration for a solution of Texas Red-cystein. Two lenses with different numerical apertures were used. It is seen that reliable diffusion times are obtained down to sample concentrations of 200 fM.

The ρ_i are the relative amplitudes corresponding to molecules with distinct diffusion coefficients; they are related to their concentrations c_i by

$$G(\tau) = \frac{1}{N} \sum_{i=1}^m \rho_i g_i(\tau) + 1 \quad (5)$$

with

$$g_i(\tau) = \left(1 + \frac{\tau}{\tau_{\text{diff},i}}\right)^{-1} \left(1 + \frac{\tau}{\tau_{\text{diff},i} K^2}\right)^{-1/2}.$$

$$\rho_i = \frac{\phi_i^2 c_i}{\sum_{i=1}^m \phi_i^2 c_i} \quad (6), \quad \text{where } \phi_i \text{ is the quantum yield of species i.}$$

2.1.3. Triplet contribution

Up to now only number fluctuations in the detection volume have been considered to contribute to the fluctuations of the light intensity at the detector, under the simplifying assumption that an excited fluorophor will emit a constant light flux. Because of the quantum nature of light and the photophysics of fluorescent molecules this is not the case. The most important effect that has to be considered is a transition of the excited molecule into the triplet state. This will 'interrupt' the stream of photons for approximately the triplet lifetime of the fluorophor and add another contribution to the autocorrelation function which - in good approximation - is then⁹:

$$G(\tau) = (1 + \beta e^{-\lambda\tau}) \left(\frac{1}{N} \sum_{i=1}^m \rho_i g_i(\tau) \right) + 1 \quad (7)$$

The amplitude of the triplet term β and its relaxation time λ increase with the excitation light intensity up to a limit given by the excitation, emission and intersystem crossing probabilities of the fluorophore. Practically, β can reach amplitudes higher than the number correlation function itself. Since relaxation time of the triplet term is of the same order as the diffusion times of small molecules (some μs), it is important to conduct the FCS experiment with a laser intensity that keeps β as small as possible.

2.1.4. Two-color cross-correlation

The detection of specific binding between biomolecules by FCS depends on a change in molecular size: when the diffusion time changes sufficiently upon binding, the complex can be distinguished in $G(\tau)$ as a second species and its concentration determined (Eqs. 5 and 6). However, in cases when the diffusion time changes only very slightly or not at all, i.e. when a non-fluorescent ligand binds to a larger fluorescent particle or in the case of exchange reactions (see below), this approach is not practicable anymore.

Recently Schwille et al. have presented a device for two-color fluorescence cross-correlation spectroscopy (FCCS)⁸. In this method the fluorescence is detected at two distinct wavelengths simultaneously in the same detection volume (Fig. 2). The signals from the two detectors are analyzed by computing their cross-correlation function. It is easily seen that in a mixture of two fluorescent molecules emitting at the two wavelengths but not interacting with each other the particles will diffuse independently and the amplitude of the cross-correlation function will be zero. On the other hand, when the particle is labeled with two dyes and emits simultaneously at the two detection wavelengths, the cross-correlation function is equal to the autocorrelation function for single-color FCS (assuming equal detection efficiencies and exact overlap of the detection volumes for the two channels). This latter case occurs when the two fluorescent species form a complex.

In FCCS, therefore, the amount of complex formation between two fluorescently labeled biomolecules can be obtained simply by measuring the cross-correlation amplitude.

2.2. Construction of a typical FCS instrument

2.2.1. The confocal setup

An inverted microscope with attached confocal optics represents a very convenient means to measure fluorescence fluctuations in a very small volume. Fig. 5 shows a picture of a setup developed in our laboratory (Tewes and Langowski, manuscript in preparation).

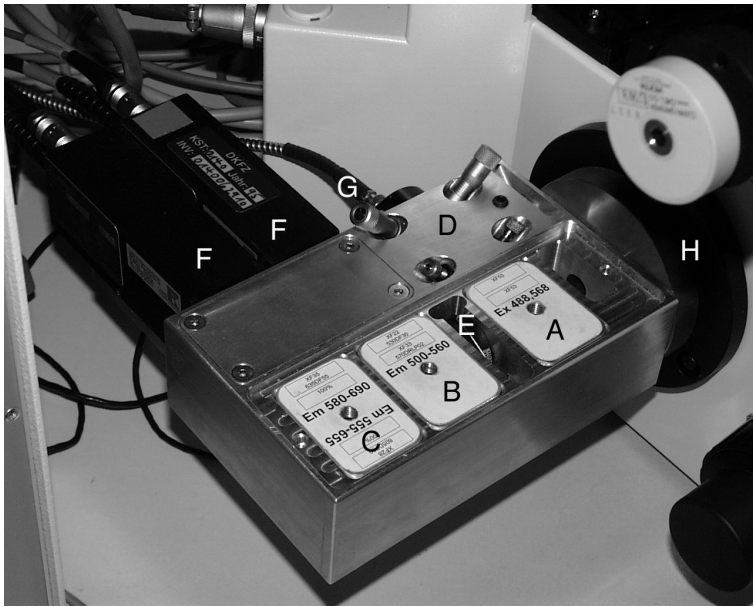


Fig. 5: Confocal FCS attachment to an inverted microscope (explanation see text).

The laser source in this case is an argon/ krypton laser coupled into a fiber which is attached to the box containing the confocal optics at G. The beam emitted from the end of the fiber is collimated and focused in D; the position of the laser focus can be adjusted in three dimensions by micrometer screws. A is a filter/ dichroic mirror combination which selects a laser wavelength and reflects it into the video port of the microscope (H). The microscope lens focuses the laser beam into the measuring cell (outside the picture), and the emitted fluorescence is

imaged by the same lens through the dichroic mirror A on the pinhole E. The laser exit point in D can be adjusted such that its image in the measuring cell coincides with that of the pinhole E (confocal condition). B and C are dichroic mirror/filter combinations which select the fluorophore emission wavelengths and image the pinhole on the active area of the avalanche photodiode single-photon detectors F. The photon pulse stream is sent to the correlation electronics, where the autocorrelation function is formed and analyzed.

2.2.2. Lenses

The microscope lenses used in FCS should be of very high numerical aperture (at least 0.9) to minimize the size of the focal volume and therefore maximize the fluctuation amplitude for a given fluorophore concentration. Some lenses used in FCS and their characteristics are described in Table 2.

The sample is generally present in aqueous solution and is observed in an inverted microscope through a standard cover slide (0.13-0.17 mm thickness).

In most cases a water immersion lens

is used because an oil immersion lens will lose focus very close (some 4 to 6 μm) above the inner surface of the cover slide. The water immersion lens has a focal spot of very high quality even at working depths of 200 μm above the cover slide surface.

The high aperture water-immersion lenses all are adjustable for varying cover slide thickness. This adjustment is important as Fig. 6 shows: while the total fluorescence intensity varies only slightly with the setting of the cover slide adjustment of the lens, this parameter has a strong effect on the number of molecules in the observation volume and on the measured diffusion time.

Some lenses exist that can be adjusted for immersion and sample fluids of varying refractive index, such as water / glycerol / sucrose solutions; such lenses have been applied successfully in FCS⁵.

Table 2: Some microscope lenses used in FCS

Type	Power	NA	characteristics
Zeiss C-APOCHROMAT	40	1.2	correction for cover glass thickness
Olympus	60	1.2	correction for cover glass thickness
Olympus	40	0.9	large working distance (2mm)

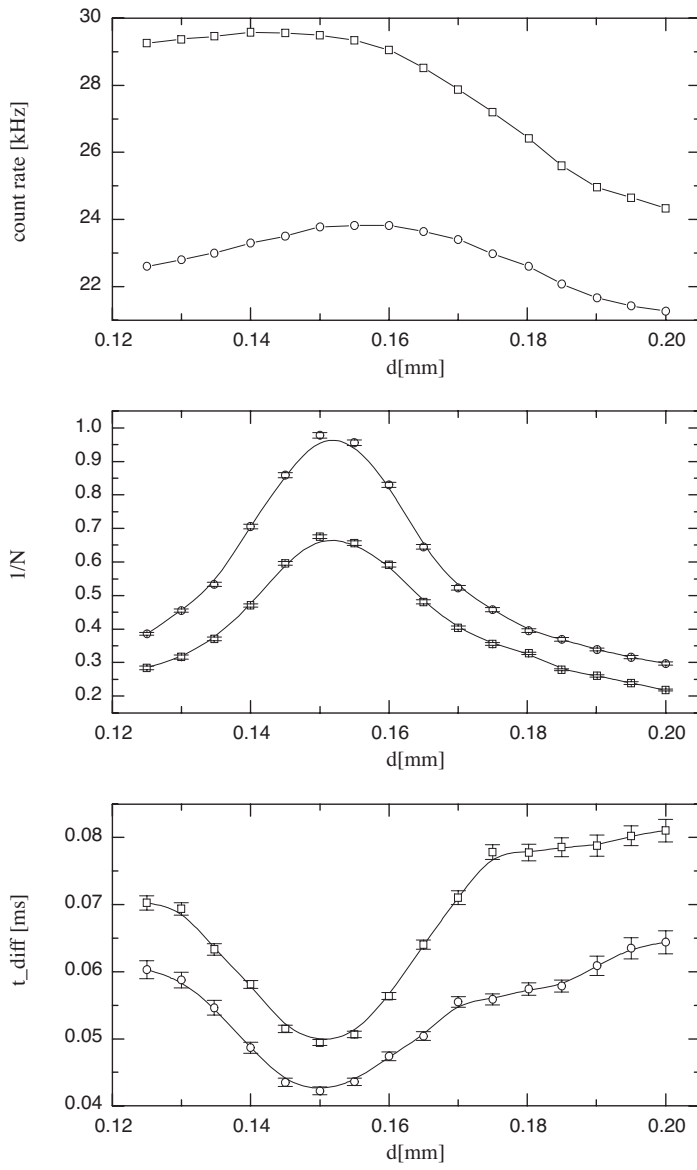


Fig. 6: effect of adjustment of cover slide thickness on the effective focal volume in FCS. The samples were 5 nM solutions of Fluorescein-cysteine (○) or Texas Red-cysteine (□).

Upper graph: measured fluorescence intensity (photon count rate in kHz), middle: reciprocal of particle number in observation volume, lower: measured diffusion time.

Table 3: Lasers applied in FCS, their powers and wavelengths

Wavelength	power (mW)	Type of laser
442	10	He/Cd
457, 488, 514	10-200	air-cooled argon ion
488, 514, 568	10-50	air-cooled argon/krypton ion
510	10-200	diode-pumped frequency-doubled Nd/YAG
543.5	1-5	green He/Ne
632.8	5-50	red He/Ne

Quebec, Canada), have a quantum yield of up to 70% at 600 nm. The advent of these devices has greatly enhanced the practicability of FCS, because very often count rates can be as low as a few hundred cps even with avalanche detectors.

2.2.3. Laser

Generally, a CW laser is used for excitation. Emission wavelengths of typical CW lasers that can be used in FCS are summarized in Table 3. The correct alignment of two excitation lasers for two-wavelength excitation into the same focal spot is a formidable mechanical problem⁸; multi-wavelength lasers, such as Ar or Ar/Kr ion lasers, offer the advantage that this alignment is avoided.

2.2.4. Optics, filters

For separating the excitation and emission wavelengths in FCS, usually dichroic beam splitters and interference filters are used. For multi-wavelength lasers the excitation wavelength is selected with a suitable bandpass filter in the excitation pathway. Even for single-wavelength lasers we found such a filter important for obtaining good results, since some parasitic light is usually present. The dichroic mirror, on the other hand, is not essential and might be replaced by a beam splitter that directs only 10% of the excitation light into the sample, because the laser power is usually not a limiting factor. The fluorescence emission is detected through a second filter which can be of the low-pass or bandpass type depending on whether the Raman scattering from water needs to be suppressed or not.

2.2.5. Detector

One of the essential components of the FCS device is a detector that registers the emitted photons with very high efficiency. Most of the dyes used in FCS emit in the yellow to red range of the spectrum, where the quantum efficiency of even red-enhanced photomultipliers is of the order of a few percent. However, recent avalanche photodiode detectors, such as the SPCM series (EG&G optoelectronics, Vaudreuil,

2.2.6. Autocorrelator

The computation of the autocorrelation function (ACF) of the fluorescent light intensity is central to the FCS experiment. Generally, the ACF is constructed from the detected photon pulses by an electronic autocorrelator. This device multiplies the number of pulses $n(t)$ counted during a time interval δt with the number $n(t-\tau)$ counted during the same interval at an earlier time, building the average $\langle n(t)n(t-\tau) \rangle$. This process is done simultaneously for a large number of different time delays τ , accumulating the ACF $G(\tau)$ in real time.

Modern autocorrelators will allow to measure the ACF simultaneously over a range of delay times of 10^{-8} s to > 1000 s, with a choice of either auto- or cross-correlation mode (e.g. ALV- 5000, ALV GmbH, Langen, Germany).

2.3. Sample requirements

The measured sample should fulfill some basic conditions for a successful FCS experiment. First, care has to be taken in the choice of the labeling dye. An obvious criterion is that its excitation and emission maxima should be compatible with the laser light source and filters used. Furthermore, many systems (such as living cells) exhibit intrinsic fluorescence which can cause artifacts; in such cases dyes are recommended that can be excited in the red part of the visible spectrum (such as Cy5). A large selection of fluorescent dyes and their derivatives can be found in the Molecular Probes catalog (Molecular Probes, Eugene, Oregon, USA).

Self-association of the dye or non-specific binding to sample impurities can lead to the formation of fluorescent aggregates. Their presence interferes with the measurement because another, usually slower component will be present in the ACF as an artifact. Self-association is especially critical with large hydrophobic fluorophores, such as Texas Red, and when the sample is labeled to a high degree, as in cross-correlation experiments where labeling of 100% of the sample molecules is necessary. In those cases, care has to be taken that the association state of the biomolecule is the same as for the non-labeled sample. This can be verified by other methods, e.g. light scattering or analytical ultracentrifugation.

3. Some examples from current research

3.1. Triplex formation

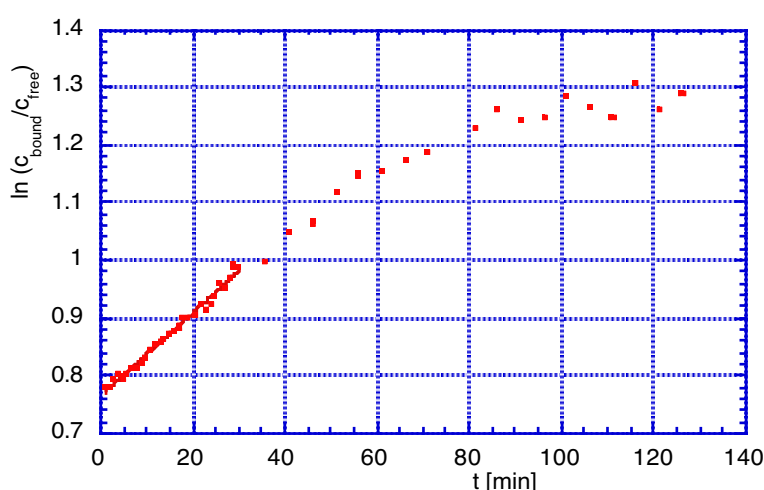


Fig. 7: binding kinetics of a rhodamine labeled triplex forming oligonucleotide to a plasmid DNA containing the complementary sequence. The association rate constant is obtained from the initial slope of a plot of $\ln(c_{\text{bound}}/c_{\text{free}})$ vs. time.

DNA triple helices can be formed by binding a single-stranded homopyrimidine sequence to a complementary homopurine-homopyrimidine duplex^{10,11}. The direct observation of this complex formation in solution has been difficult because of the lack of an optical signal which could be used for its detection. FCS is a very convenient means for studying the binding thermodynamics and kinetics of triplex formation, because the complex has a significantly smaller diffusion coefficient than the free ligand. Thus, two relaxation times can be distinguished in a mixture of complex and free ligand and the relative amounts quantified. Because

FCS is relatively fast, the kinetics of complex formation can be observed on a time scale of minutes.

In a recent study (Pfannschmidt and Langowski, manuscript in preparation), triplex formation was studied on the 27 bp sequence 3'-TTCCTCCTTCCTTCCTTCCTCCC-5' contained in a 2.5 kbp superhelical plasmid. The complementary triplex-forming oligonucleotide (TFO) had the same sequence in opposite direction and was rhodamine-labeled at the 5'-end. The measurements were done in 10 mM sodium acetate, 50 mM MgCl₂, 0.01% NP-40 at pH values between 4.0 and 7.0.

Here we used a Zeiss/Evotec Confocor FCS spectrometer with an excitation wavelength of 488 nm. The diffusion times of the free oligonucleotide and of the complex were sufficiently different that the two components of the autocorrelation function could be separated. The free TFO had a diffusion time between 140 and 200 μ s and the complex between 3.56 and 4.25 ms. These variations are due to the alignment of the instrument, which had to be repeated before each set of measurements; the ratio of the diffusion times for the TFO and for rhodamine was constant within $\pm 3\%$. The change in quantum yield upon binding was determined separately to $Q_{\text{bound}}/Q_{\text{free}} = 0.35$.

The binding kinetics of the rhodamine-TFO to the plasmid DNA are shown in Fig. 7. It is evident that the quantum yield of the bound TFO has a large influence on the measured degree of binding and must be considered in the evaluation of the data. Association rate constants k_1 were determined by a fit to the initial slope of the plot and the binding constant K_{ass} from its plateau for large times; the dissociation rate constant k_{-1} was calculated from K_{ass} and k_1 . We found $k_1 = 3.3 \cdot 10^3 \text{ l mol}^{-1} \text{ s}^{-1}$, $K_{\text{ass}} = 1.54 \cdot 10^8 \text{ l mol}^{-1}$, and $k_{-1} = 2.14 \cdot 10^{-5} \text{ s}^{-1}$ at pH=7.0.

3.2. NtrC protein

NtrC (nitrogen regulatory protein C) from enteric bacteria is a transcription factor that activates a variety of genes that are involved in nitrogen utilization by contacting simultaneously a binding site on the DNA and RNA polymerase complexed with the σ^{54} sigma factor at the promoter. The NtrC binding sites found *in vivo* are several hundred base pairs upstream from the promoter, and activation requires looping of the intervening DNA for interaction with RNAP- σ^{54} .

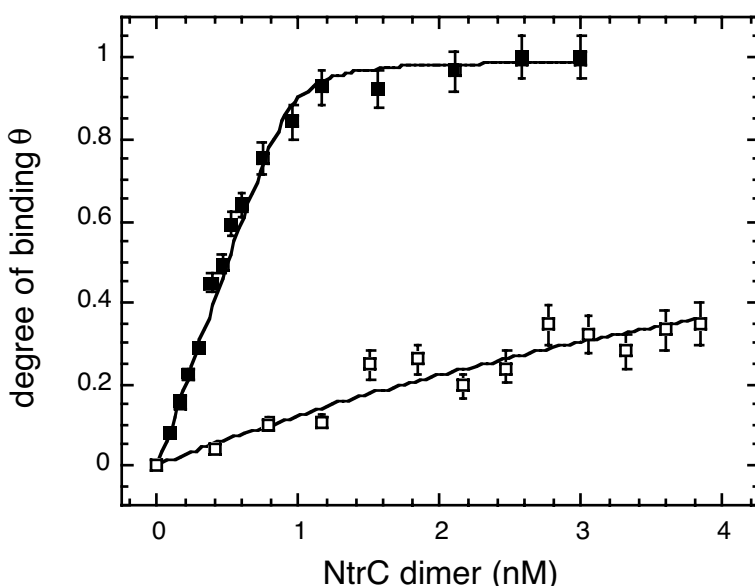


Fig. 8: FCS titration curves for NtrC (■) at 15 mM KCl, (□) at 600 mM KCl. The lines are theoretical binding curves for a 1:1 complex fitted to the experimental data.

NtrC is a dimer in solution and binds as a dimer to a single binding site as demonstrated recently by analytical ultracentrifugation¹². While the latter technique is a useful tool for determining the binding stoichiometry, the binding constant is too high under physiological conditions to be determined at the protein and DNA concentrations used in ultracentrifugation. FCS has been used recently¹³ to measure the binding constant of NtrC to a fluorescently labeled oligonucleotide at low ionic strengths where the binding is very strong and consequently has to be measured at very low concentrations.

An oligonucleotide was used that contained the NtrC binding site and was labeled with tetramethylrhodamine at the 5' end of one strand. First the diffusion time τ_1 , the structure factor κ , the triplet

relaxation time λ , and the triplet amplitude β were determined for free DNA in the absence of protein ($\theta = 0$). At saturating protein concentrations ($\theta = 1$) the diffusion time τ_2 of the protein-DNA complex could be measured. The ratio of diffusion times τ_1 and τ_2 of the two species is equal to the ratio of their translational diffusion constants D_1 and D_2 :

$$\frac{\tau_2}{\tau_1} = \frac{D_1}{D_2} \quad (8)$$

Knowing the ratio τ_1/τ_2 which is constant, and the diffusion time of the free DNA, τ_1 , which is calibrated for each experiment, enables one to determine the relative amplitude of the two components with diffusion times τ_1 and τ_2 in the measured autocorrelation function, corresponding to free and complexed DNA. Fig 8 shows a plot of the relative amount of bound DNA as a function of free protein concentration from which the binding constant was determined by fitting a standard binding curve.

We found $K_{ass} = (7.1 \pm 2.5) \cdot 10^{10} \text{ M}^{-1}$ at 15 mM KCl and $K_{ass} = (1.4 \pm 0.4) \cdot 10^8 \text{ M}^{-1}$ at 600 mM KCl. This result shows that the binding constant is strongly salt dependent and can be interpreted by the formation of two ion pairs upon binding of an NtrC dimer to DNA¹³.

From the cited ultracentrifugation studies¹² it has been suggested that one NtrC octamer can bind two DNA double strands simultaneously on independent binding sites. This can also be shown directly by FCCS. When NtrC protein is added to a 1:1 mixture of fluorescein- and tetramethylrhodamin-labeled oligonucleotide containing the specific binding site, a significant increase in the cross correlation amplitude is seen which reaches its saturation at a stoichiometry of 2 oligonucleotides per NtrC. The maximum cross correlation amplitude is exactly that expected when 50% of the complexes carry one fluorescein- and one rhodamin-labeled DNA, and 25% each carry two DNAs of the same kind; this ratio is expected simply from statistics.

3.3. Vimentin oligomerization

Vimentin is one of the major protein components of the cytoskeleton of eukaryotic cells. One of its essential properties is the formation of intermediate filaments through self-association. The first step of this reaction is a dimerization where two protein monomers associate side by side to form an elongated rod; the formation of tetramers from two dimers is generally assumed to be the next step. Using FCS one can decide whether the protein forms a dimer or a tetramer in solution, and whether subunits can exchange between the complexes.

3.3.1. Stoichiometry of vimentin oligomers

The simplest method for determining the number of proteins per vimentin oligomer is to compare the mean count rate per particle for oligomers and monomers. However, vimentin forms monomers only at very high urea concentrations (8M), and the FCS measurement becomes problematic because of the high refractive index of the urea solution. A comparison with free dye is imprecise because the quantum yields of the labeled protein and the free dye may be different. Therefore we used as a reference a solution of vimentin oligomers that had been reconstituted by dialysis from a mixture of 98% unlabeled and 2% labeled protein in 8M urea. In this solution the majority of the labeled oligomers will carry only one labeled vimentin. The average fluorescence intensity (count rate) per molecule can be computed for this reference and the fully labeled sample by normalizing the integrated fluorescence intensity $\langle F \rangle$ with the average number of particles in the detection volume, $\langle N \rangle$, and the oligomerization stoichiometry n is then obtained as

$$n = \frac{\langle F_{sample} \rangle / \langle N_{sample} \rangle}{\langle F_{ref} \rangle / \langle N_{ref} \rangle} \quad (9)$$

In the case of vimentin in 5 mM Tris HCl, 1 mM EDTA, 0.005% Tween 20, pH 9.5 (low salt buffer), a stoichiometry of $n = 2.2 \pm 0.1$ was obtained, indicating that vimentin is a dimer under these conditions.

3.3.2. Exchange of vimentin monomers measured by FCCS

For detecting the exchange of vimentin monomers between dimers in solution, FCCS can be used very conveniently. The strategy of the measurement is to prepare vimentin samples labeled with either fluorescein (F-vimentin) or Texas Red (TR-vimentin), mix equal amounts of the two samples and measure the FCCS cross-correlation function (CCF).

As outlined above, the amplitude of the CCF will be zero for non-interacting molecules (except for crosstalk between the detection channels, which cannot be completely avoided) because their diffusion is uncorrelated. When an exchange takes place, dimers will form which contain both fluorophors and the CCF

amplitude will increase in proportion to their concentration.

In the experiment a 1:1 mixture of F- and TR-vimentin was incubated for 10 min at various temperatures, then cooled to room temperature and measured in the FCCS with detection channels for fluorescein and Texas Red emission. Fig. 8 shows the ratio of CCF to ACF amplitudes as a function of incubation temperature. The reference line is the ratio that is obtained from a 1:1 mixture of F- and TR-vimentin monomers in 8M urea that was dialyzed against low salt buffer to form mixed dimers. It is clearly seen that the proportion of mixed dimer as detected in the CCF increases with temperature, and reaches the maximum value at 70 °C.

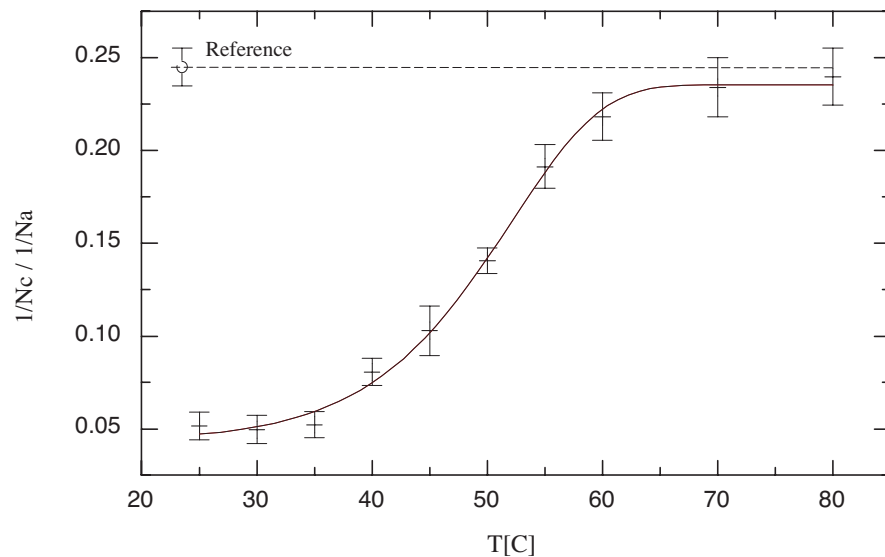


Fig. 9: Amplitude of the fluorescence cross-correlation function between the fluorescein and Texas Red channels for mixtures of fluorescein- and Texas Red-labeled vimentin dimers which had been incubated for 10 min at various temperatures. The reference line gives the value expected for complete exchange, measured on a sample that had been mixed in 8M urea and then dialyzed to form dimers.

°C.

3.4. Intracellular motions

FCS can also be used to study the motion of fluorescent probes inside living cells. The probe can either be a fluorescent component that is brought into the cell by simple diffusion or microinjection. Alternatively, a variety of fluorescent proteins exist that can be cloned and expressed inside the cell. Green fluorescent protein (GFP) is the most commonly known, but variants thereof exist, such as yellow, cyan, blue, and enhanced green fluorescent proteins (YFP, CFP, BFP, EGFP).

For testing models of the intranuclear distribution of chromatin and chromosomes, we have investigated the spatial variations of the diffusion behavior of a green fluorescent protein mutant EGFP (F64L/S65T) and of an EGFP-β-galactosidase fusion protein in living cells with FCS. While diffusion in the cytoplasm appears to be unrestricted and is governed by a simple random walk behavior, the diffusion in the nucleus can be

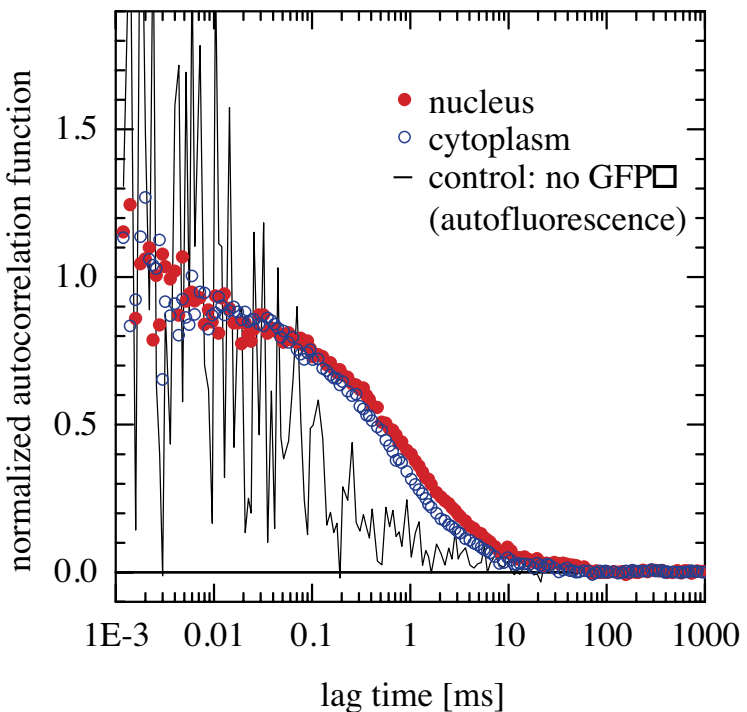


Fig. 10: FCS autocorrelation functions of EGFP inside the nucleus and cytoplasm of COS-7 cells.

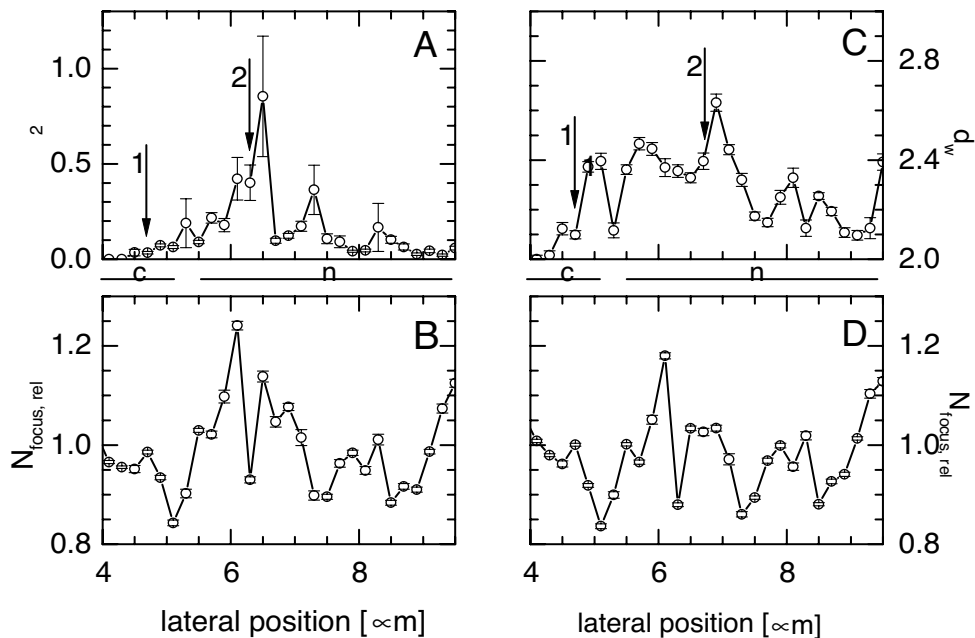


Fig. 11: lateral FCS scans through EGFP-expressing COS-7 cells evaluated using a two-component model (left, A and B) or the anomalous diffusion model (right, C and D).

concentration of 60 nM EGFP. The regions marked **c** and **n**, and arrows 1 and 2, correspond to the cytoplasm and the nucleus, respectively. It can be seen that the amplitude of the slow component, respectively the obstacle density, increases in the nucleus relative to the cytoplasm. This probably indicates crowding of the nuclear space by the interphase chromosomes. Work is in progress in our group that relates the anomalous diffusion parameter d_w to the fractal dimension and the density of the chromatin fiber network as predicted from polymer models of interphase chromosomes 14,15.

described by an anomalous diffusion process that is characterized by $\langle x^2 \rangle = 6Dt(\tau_0)^{\alpha-1}$ with $\alpha < 1$. This behavior is in agreement with theories that describe diffusion in the presence of obstacles and polymer chain models of the interphase nucleus. Fig. 10 shows FCS autocorrelation functions taken in the cytoplasm and the nucleus of an EGFP-expressing COS-7 cell. It is evident that the decay in the nucleus is slower than in the cytoplasm, indicating a restricted mobility of the protein in the nucleus. The FCS data can be evaluated either with a simple two-component model where a fast component corresponds to unrestricted diffusion of the protein and a slow component ρ_2 to a bound or trapped protein fraction (Fig. 11 left, graphs A and B), or by an anomalous diffusion model where the protein moves through a network of obstacles and d_w is a parameter related to the obstacle density (right, graphs C and D). N indicates the normalized average number of particles inside the focal volume of the microscope; a value of 1 corresponds to a concen-

References

1. Elson, E. L. & Magde, D. Fluorescence correlation spectroscopy. I. Conceptual basis and theory. *Biopolymers* **13**, 1-27 (1974).
2. Magde, D., Elson, E. L. & Webb, W. W. Fluorescence correlation spectroscopy. II. An experimental realization. *Biopolymers* **13**, 29-61 (1974).
3. Webb, W. W. Applications of fluorescence correlation spectroscopy. *Q Rev Biophys* **9**, 49-68 (1976).
4. Qian, H. & Elson, E. L. Analysis of Confocal Laser-Microscope Optics for 3-D Fluorescence Correlation Spectroscopy. *Applied Optics* **30**, 1185-1195 (1991).
5. Rigler, R., Mets, Ü., Widengren, J. & Kask, P. Fluorescence correlation spectroscopy with high count rate and low background: analysis of translational diffusion. *Eur. Biophys. J.* **22**, 169-175 (1993).
6. Sorscher, S. M., Bartholomew, J. C. & Klein, M. P. The use of fluorescence correlation spectroscopy to probe chromation in the cell nucleus. *Biochim. Biophys. Acta* **610**, 28-46 (1980).
7. Ricka, J. & Binkert, T. Direct measurement of a distinct correlation function by fluorescence cross correlation. *Phys. Rev. A* **39**, 2646-2652 (1989).
8. Schwille, P., Meyer-Almes, F. J. & Rigler, R. Dual-color fluorescence cross-correlation spectroscopy for multicomponent diffusional analysis in solution. *Biophysical Journal* **72**, 1878-1886 (1997).
9. Widengren, J., Mets, Ü. & Rigler, R. Fluorescence Correlation Spectroscopy of Triplet States in Solution: A Theoretical and Experimental Study. *J. Phys. Chem.* **99**, 13368-13379 (1995).
10. Wells, R. D., Collier, D. A., Hanvey, J. C., Shimizu, M. & Wohlrab, F. The chemistry and biology of unusual DNA Strucutures adopted by oligopurine-oligopyrimidine sequences. *FASEB J.* **2**, 2939-2949 (1988).
11. Hélène, C. & Toulmé. in *Oligodeoxynucleotides: Antisense Inhibitors of Gene Expression* (ed. Cohen, J. S.) 139ff (Macmillan Press 1989, 1989).
12. Rippe, K., Mücke, N. & Schulz, A. Association states of *E. coli* NtrC protein determined by analytical ultracentrifugation. *Journal of Molecular Biology* **278**, 915-933 (1998).
13. Sevenich, F. W., Langowski, J., Weiss, V. & Rippe, K. DNA binding and oligomerization of NtrC studied by fluorescence anisotropy and fluorescence correlation spectroscopy. *Nucleic Acids Research* **26**, 1373-1381 (1998).
14. Münkel, C. & Langowski, J. Chromosome structure described by a polymer model. *Physical Review E* **57**, 5888-5896 (1998).
15. Münkel, C. et al. Compartmentalization of interphase chromosomes observed in simulation and experiment. *Journal of Molecular Biology* **285**, 1053-1065 (1999).

Some introductory remarks about Brownian motion and FCS theory

Jörg Langowski, DKFZ Heidelberg, Division Biophysics of Macromolecules
joerg.langowski@dkfz.de

1. Diffusion equation, Smoluchowski equation

Fick's first law:

$$\mathbf{j} = -D \operatorname{grad} c \quad (1.1)$$

Continuity equation:

$$\frac{\partial c}{\partial t} = -\operatorname{div} \mathbf{j} \quad (1.2)$$

Combining (1.1) and (1.2) we obtain Fick's second law:

$$\frac{\partial c}{\partial t} = \operatorname{div} \operatorname{grad} c \quad (1.3)$$

This is correct as long as no external forces act on the particles, i.e. their potential energy is position-independent. In the presence of an external potential $U(\mathbf{r})$, the corresponding force $\mathbf{F} = -\operatorname{grad} U$ will induce a velocity $\mathbf{v} = \mathbf{F}/\gamma$ where γ is the friction factor of the particle:

$$\mathbf{v} = -\frac{1}{\gamma} \operatorname{grad} U \quad (1.4)$$

This velocity induces an additional flux $\mathbf{j}_v = c \mathbf{v}$. Thus, eq. (1.1) becomes

$$\mathbf{j} = -D \operatorname{grad} c - \frac{c}{\gamma} \operatorname{grad} U \quad (1.5)$$

At equilibrium, the flux vanishes and the concentration follows a Boltzmann distribution with regard to the potential U , therefore

$$D \operatorname{grad} e^{-\frac{U(\mathbf{r})}{k_B T}} = -\frac{1}{\gamma} e^{-\frac{U(\mathbf{r})}{k_B T}} \operatorname{grad} U \quad (1.6)$$

which is the same as

$$-\frac{D}{k_B T} e^{-\frac{U(\mathbf{r})}{k_B T}} \operatorname{grad} U = -\frac{1}{\gamma} e^{-\frac{U(\mathbf{r})}{k_B T}} \operatorname{grad} U \quad (1.7)$$

from which it follows immediately that

$$D = \frac{k_B T}{\gamma} \quad (1.8)$$

which is Einstein's relationship between the diffusion coefficient of a particle and its friction factor.

The *Smoluchowski equation* for the diffusion in the presence of an external potential can be obtained from eqs.(1.5), (1.8) and the continuity equation (1.2):

$$\frac{\partial c}{\partial t} = \operatorname{div} \left[\frac{1}{\gamma} (k_B T \operatorname{grad} c + c \operatorname{grad} U) \right] \quad (1.9)$$

2. Fluctuation-dissipation theorem

We start with the Langevin equation for the velocity of a particle of mass m and friction factor γ :

$$m\mathbf{v}(t) = \mathbf{F}(t) - \boldsymbol{\gamma}(t) \quad (2.1)$$

The formal solution for this equation is (setting $\beta = \gamma/m$):

$$\mathbf{v}(t) = \mathbf{v}(0)e^{-\beta t} + \int_0^t \mathbf{F}(\tau) e^{-\beta(t-\tau)} d\tau \quad (2.2)$$

Multiplying both sides with $\mathbf{v}(0)$ and averaging leads to:

$$\langle \mathbf{v}(0)\mathbf{v}(t) \rangle = \langle \mathbf{v}(0)\mathbf{v}(0) \rangle e^{-\beta t} + \int_0^t \langle \mathbf{v}(0)\mathbf{F}(\tau) \rangle e^{-\beta(t-\tau)} d\tau \quad (2.3)$$

We can show that $\mathbf{v}(0)$ and $\mathbf{F}(t)$ are uncorrelated; therefore the term under the integral becomes zero and we obtain simply

$$\langle \mathbf{v}(0)\mathbf{v}(t) \rangle = \langle \mathbf{v}(0)^2 \rangle e^{-\beta t} \quad (2.4)$$

This is the *velocity autocorrelation function* of the particle.

The mean square displacement of a particle with diffusion coefficient D in a three-dimensional random walk is

$$\langle R^2 \rangle = 6Dt \quad (2.5)$$

and is also related to the velocity autocorrelation function by

$$\begin{aligned} R(t) &= \int_0^t \mathbf{v}(\tau) d\tau \\ \langle R^2(t) \rangle &= \int_0^t \int_0^t \langle \mathbf{v}(t_1) \mathbf{v}(t_2) \rangle dt_1 dt_2 \end{aligned} \quad (2.6)$$

We then assume that $\langle \mathbf{v}(t_1) \mathbf{v}(t_2) \rangle = \langle \mathbf{v}(0) \mathbf{v}(t_2 - t_1) \rangle$; $\langle \mathbf{v}(0) \mathbf{v}(t) \rangle|_{t \rightarrow \infty} = 0$; $\langle \mathbf{v}(0) \mathbf{v}(t) \rangle = \langle \mathbf{v}(0) \mathbf{v}(-t) \rangle$ and obtain after integration by parts

$$\langle R^2(t) \rangle = 2 \int_0^t (t - \tau) \langle \mathbf{v}(0) \mathbf{v}(\tau) \rangle d\tau \quad (2.7)$$

With eq. (2.5) we obtain

$$D = \frac{1}{3t} \int_0^t (t-\tau) \langle \mathbf{v}(0)\mathbf{v}(\tau) \rangle d\tau \quad (2.8)$$

For $t \rightarrow \infty$ the velocity autocorrelation function is zero (eq.(2.4)), and the integral simplifies to

$$D = \frac{1}{3} \int_0^\infty \langle \mathbf{v}(0)\mathbf{v}(\tau) \rangle d\tau \quad (2.9)$$

This is a so-called *Green-Kubo relationship* that connects the autocorrelation function of a fluctuating quantity with a transport coefficient.

Now the mean kinetic energy of the particle is $\frac{m}{2}\langle \mathbf{v}^2 \rangle = \frac{3}{2}k_B T$ in thermodynamic equilibrium (according to the equipartition theorem); this is related to the area under the velocity autocorrelation function by

$$\int_0^\infty \langle \mathbf{v}(0)\mathbf{v}(\tau) \rangle d\tau = \langle \mathbf{v}(0)^2 \rangle \int_0^\infty e^{-\beta\tau} d\tau = \frac{3k_B T}{m} \cdot \frac{m}{\gamma} \quad (2.10)$$

and therefore, with (2.9), we obtain again the Einstein relationship, $D = k_B T / \gamma$ (eq.(1.8)).

(Note: The energy dissipated per unit time by a particle dragged through a viscous medium with force \mathbf{F} and velocity $v = F/\gamma$ is $E = F \cdot v = F^2/\gamma$. Thus, eq. (2.9) relates the fluctuation of a dynamic quantity (velocity) with the energy dissipated by this quantity; it is an expression of a more general law of statistical physics called the *fluctuation-dissipation theorem*. Similar relationships can be set up for other quantities, e.g. voltage U and resistance R : $E = U^2/R$).

We can also get to the Green-Kubo relationship through the following route. Starting again with the Langevin equation, $m\dot{\mathbf{v}}(t) = \mathbf{F}(t) - \gamma\mathbf{v}(t)$, and forming correlation functions by averaging over the product of both sides with $\mathbf{v}(t+\tau)$, we get:

$$m\langle \mathbf{v}(t)\mathbf{v}(t+\tau) \rangle = -\gamma\langle \mathbf{v}(t)\mathbf{v}(t+\tau) \rangle + \langle \mathbf{F}(t)\mathbf{v}(t+\tau) \rangle \quad (2.11)$$

$\mathbf{F}(t)$ and $\mathbf{v}(t+\tau)$ are uncorrelated (see above); integrating both sides gives

$$m \int_0^\infty \langle \mathbf{v}(t)\mathbf{v}(t+\tau) \rangle d\tau = -\gamma \int_0^\infty \langle \mathbf{v}(t)\mathbf{v}(t+\tau) \rangle \quad (2.12)$$

which is completely equivalent to

$$m \int_0^\infty \langle \mathbf{v}(t)\mathbf{v}(t+\tau) \rangle d\tau = -\gamma \int_0^\infty \langle \mathbf{v}(t)\mathbf{v}(t+\tau) \rangle \quad (2.13)$$

(here the dot denotes the derivative with respect to τ), and then the left hand integral can be executed as:

$$\begin{aligned}
m \int_0^\infty \langle \mathbf{v}(t) \mathbf{v}(t + \tau) \rangle d\tau &= m \langle \mathbf{v}(t) \mathbf{v}(t + \tau) \rangle |_0^\infty = \\
&= -m \langle \mathbf{v}^2 \rangle = -\gamma \int_0^\infty \langle \mathbf{v}(t) \mathbf{v}(t + \tau) \rangle
\end{aligned} \tag{2.14}$$

As before, we set $m \langle \mathbf{v}^2 \rangle = 3k_B T$ and obtain

$$\frac{k_B T}{\gamma} = -\frac{1}{3} \int_0^\infty \langle \mathbf{v}(t) \mathbf{v}(t + \tau) \rangle \tag{2.15}$$

Using the Einstein relationship, this is the same as eq.(2.9).

We can also obtain a general expression for the mean squared displacement of a Brownian particle for all times t. Using eq.(2.4), eq.(2.7), and $m \langle \mathbf{v}^2 \rangle = 3k_B T$ we get

$$\langle R^2(t) \rangle = \frac{6k_B T}{m} \int_0^t (t - \tau) e^{-\beta\tau} d\tau \tag{2.16}$$

which integrated out gives

$$\langle R^2(t) \rangle = 6D \left[t + \frac{1}{\beta} (e^{-\beta t} - 1) \right] \tag{2.17}$$

For $t \gg \beta^{-1}$, this reduces to $\langle R^2 \rangle = 6Dt$, the known expression for the random walk. Expanding the exponential at $t \rightarrow 0$ we get

$$\begin{aligned}
\langle R^2(t) \rangle &\approx 6D \left[t + \frac{1}{\beta} (1 - \beta t + \frac{1}{2} \beta^2 t^2 - 1) \right] = \\
&= \frac{6D}{\beta} \cdot \frac{1}{2} \beta^2 t^2 = \frac{3k_B T}{m} t^2 = \langle \mathbf{v}^2 \rangle t^2
\end{aligned} \tag{2.18}$$

In this case, the displacement is linear in t as would be expected for short times.

3. Fluorescence correlation spectroscopy: diffusion of particles in the Gaussian beam profile of a laser focus

Fluorescence intensity fluctuations in the detection volume V:

$$\delta F(t) = \kappa \cdot Q \cdot \int_V I_{ex}(\vec{r}) \cdot CEF(\vec{r}) \cdot \delta C(\vec{r}, t) dV \tag{3.1}$$

k: efficiency of the photodetector; Q: quantum yield of fluorophor; $I_{ex}(\mathbf{r})$: excitation intensity profile; $CEF(\mathbf{r})$: collection efficiency function of detection optics

$$E(\vec{r}) = \kappa \cdot Q \cdot I_{ex}(\vec{r}) \cdot CEF(\vec{r}) \propto e^{-2 \left(\frac{x^2 + y^2}{w_0^2} + \frac{z^2}{z_0^2} \right)} \tag{3.2}$$

(CEF and beam profile are Gaussian with profile width w_0 and length z_0)

Thus, eq. (3.1) becomes

$$\delta F(t) = \int_V E(\vec{r}) \delta c(\vec{r}, t) dV \quad (3.3)$$

The autocorrelation function of the detected fluorescence intensity is

$$G(\tau) = \frac{\langle \delta F(t + \tau) \delta F(t) \rangle}{\langle F(t) \rangle^2} \quad (3.4)$$

and with eq. (3.3) becomes

$$G(\tau) = \frac{\iint_{VV'} E(\vec{r}) E(\vec{r}') \langle \delta c(\vec{r}, 0) \delta c(\vec{r}', \tau) \rangle dV dV'}{\left(\langle c \rangle \int_V E(\vec{r}) dV \right)^2} \quad (3.5)$$

The autocorrelation function of the concentration fluctuations $\langle \delta c(\vec{r}, 0) \delta c(\vec{r}', \tau) \rangle$ can be obtained from the diffusion equation:

$$\begin{aligned} \langle \delta c(\vec{r}, 0) \delta c(\vec{r}', \tau) \rangle &= \frac{\langle \delta c(\vec{r}, 0)^2 \rangle}{(4\pi D\tau)^{3/2}} e^{-\frac{-(\vec{r}-\vec{r}')^2}{4D\tau}} \\ &= \frac{\langle c \rangle}{(4\pi D\tau)^{3/2}} e^{-\frac{-(\vec{r}-\vec{r}')^2}{4D\tau}} \quad (\text{since } \delta c^2 = c) \end{aligned} \quad (3.6)$$

Eqs. (3.5) and (3.6) yield

$$G(\tau) = \frac{\langle c \rangle}{(4\pi D\tau)^{3/2}} \frac{\int_V E(\vec{r}) \int_{V \otimes} E(\vec{r}') e^{-\frac{-(\vec{r}-\vec{r}')^2}{4D\tau}} dV' dV}{\left\langle c \int_V E(\vec{r}) dV \right\rangle^2} \quad (3.7)$$

and this can be integrated for the x, y and z components using

$$\int_{-\infty}^{\infty} e^{-\frac{2x^2}{w_0^2}} \int_{-\infty}^{\infty} e^{-\frac{2x'^2}{w_0^2} - \frac{(x-x')^2}{4D\tau}} dx' dx = w_0^2 \pi \sqrt{\frac{D\tau}{4D\tau + w_0^2}} \quad (3.8)$$

to yield the FCS autocorrelation function

$$G(\tau) = \frac{1}{\langle c \rangle V_{eff}} \frac{1}{\left(1 + \frac{4D\tau}{w_0^2} \right) \sqrt{1 + \frac{4D\tau}{\kappa^2 w_0^2}}} \quad (3.9)$$

Here $V_{\text{eff}} = \pi^{3/2} w_0^2 z_0$ is an ‘effective detection volume’ and $\kappa = z_0/w_0$ the ‘structure factor’, the axial ratio of the detection focal volume. Finally, since $\langle c \rangle V_{\text{eff}}$ is equal to the average number of particles N in the detection volume, and defining the ‘diffusion time’ $\tau_D = w_0^2/4D$ (the mean time the particle remains in the focal volume), we get:

$$G(\tau) = \frac{1}{N} \frac{1}{\left(1 + \frac{\tau}{\tau_D}\right) \sqrt{1 + \frac{\tau}{\kappa^2 \tau_D}}} \quad (3.10)$$

For an M -component mixture, $G(t)$ becomes a weighted sum with terms corresponding to the different diffusion times $\tau_{D,i}$:

$$G(\tau) = \frac{1}{N} \sum_{i=1}^M \frac{a_i}{\left(1 + \frac{\tau}{\tau_{D,i}}\right) \sqrt{1 + \frac{\tau}{\kappa^2 \tau_{D,i}}}} \quad (3.11)$$